Conference on Modelling Fluid Flow (CMFF'12)
The 15th International Conference on Fluid Flow Technologies
Budapest, Hungary, September 4-7, 2012

NUMERICAL ANALYSIS OF A SWIRLING FLOW GENERATED AT LOWER RUNNER SPEEDS

Alin I. BOSIOC[1], Constantin TANASA[2], Romeo F. SUSAN-RESIGA[3], Sebastian MUNTEAN[4], Ladislau VÉKÁS[5]

[1] Corresponding Author, PhD Eng., Romanian Academy – Timisoara Branch, Center for Fundamental and Advanced Technical Research, Bv. Mihai Viteazu 24, 300223, Timisoara, ROMANIA, Phone/Fax: +40256403692 , E-mail: alin@mh.mec.upt.ro
[2] PhD Student, Politehnica University of Timisoara, Department of Hydraulic Machinery, Bv. Mihai Viteazu 1, 300222, Timisoara, ROMANIA, Phone/Fax: +40256403692 ,E-mail: costel@mh.mec.upt.ro
[3] PhD Eng, Professor, Politehnica University of Timisoara, Department of Hydraulic Machinery, Bv. Mihai Viteazu 1, 300222, Timisoara, ROMANIA, Phone/Fax: +40256403692 ,E-mail: resiga@mh.mec.upt.ro
[4] PhD Eng., Senior Researcher, Romanian Academy – Timisoara Branch, Center for Fundamental and Advanced Technical Research, Bv. Mihai Viteazu 24, 300223, Timisoara, ROMANIA, Phone/Fax: +40256403692, E-mail: seby@acad-tim.tm.edu.ro
[5] PhD Phys., Senior Researcher, Romanian Academy – Timisoara Branch, Center for Fundamental and Advanced Technical Research, Bv. Mihai Viteazu 24, 300223, Timisoara, ROMANIA, Phone/Fax: +40256403700 , E-mail: vekas.ladislau@gmail.com

ABSTRACT

The paper focuses on numerical evaluation of energetic and hydrodynamic behaviour downstream to the runner of the swirling apparatus for lower runner speeds. The energetic behaviour of the runner consists in the analysis of the torque and mechanical power, while from the hydrodynamic behaviour is analysed the velocity field configuration downstream to it. Firstly, three-dimensional steady turbulent flow is performed along to the swirl apparatus geometry. The mixing interface method is used in order to couple the non-rotating three-dimensional domain with three-dimensional runner computational domain. As a result, only one guide vane channel and one runner interblade channel are selected. Secondly, the computation of the runner at different speeds is performed. Then, the hydrodynamic behaviour of velocity profiles (circumferential and meridian components) is analysed in order to evaluate the swirl configuration and correlate with the velocity profiles from a real runner at the outlet.

Keywords: numerical simulation, swirl generator, lower runner speeds

NOMENCLATURE

P	$[W]$	mechanical power
M	$[Nm]$	torque
n	$[rpm]$	runner speed
η	$[\%]$	hydraulic efficiency
ρ	$[kg/m^3]$	density
V_{1r}, V_{2z}	$[m/s]$	axial velocity component upstream and downstream the runner
$V_{1\theta}$, $V_{2\theta}$	$[m/s]$	circumferential velocity component upstream and downstream the runner
φ	[-]	discharge coefficient
m_2	[-]	flux of moment of momentum coefficient
R_{ref}	$[m]$	reference radius (the radius from the shroud of the free runner)
v_{sf}	[-]	swirl-free velocity component

Subscripts and Superscripts

ref	reference
sf	swirl free

1. INTRODUCTION

When the hydraulic turbines (especially, turbine with fixed blades like Francis turbines) operate at partial discharge, the decelerated swirling flow downstream the runner becomes highly unstable. Consequently, a spiral vortex breakdown (also known as pressing vortex rope in the engineering literature) is developed. The flow unsteadiness from the draft tube cone leads to severe pressure fluctuations that hinder the turbine operation.

Based on the large experience accumulated over the decades of the design process, the hydraulic losses are smaller along to the upstream

hydraulic passage of the hydraulic turbines (from the spiral casing to the runner) with respect to the draft tube. However, the hydraulic losses still exhibit large variations during the full operating range. The major energy losses are located in the draft tube according to Vu and Retieb [1]. Also, this is reflected by the Francis turbine hill chart, when the turbine is operated far from best efficiency point, its losses increase sharply with a corresponding decrease in overall efficiency. This is the reason why researchers concentrate their efforts to improve the draft tube cone flow.

An experimental test rig was developed in our laboratory in order to investigate the decelerated swirling flow unsteadiness [2]. The test rig is used to determine the parameters of the swirling flow with vortex rope. Also, different methods to control the vortex rope are evaluated in order to mitigate the pressure fluctuations, [3], [4]. The main component of the test rig is the swirl apparatus with two parts: the swirl generator and the test section similar with the draft tube cone. The swirl generator from our test rig has two blade rows. The upstream non-rotating blades (guide vanes) produce a free-vortex tangential component, while keeping the axial velocity practically constant. The second row of rotating blades (free runner) is used to create a specific energy deficit near the hub with a corresponding excess near the shroud [3]. The runner spins at the runaway speed, acting as a turbine near the hub and as a pump near the shroud, with vanishing overall torque, [5].

By reducing the speed of the runner of the swirling apparatus, is obtained the same velocity field with a Francis turbine runner operated at constant guide vane opening (with different discharges and heads).

2. SWIRLING FLOW GENERATOR AND EXPERIMENTAL TEST RIG

Two different methods are usually employed to generate a swirling flow in the laboratory conditions: using a turbine model or a swirl generator. Using a turbine model is quite expensive. Alternatively, a swirl generator is a simpler solution allowing physical phenomena investigation. For producing a swirling flow, Kurokawa et al. [6] uses an axial flow impeller at about 3.3*d* upstream of the diffuser inlet, where *d(=156 mm)* is the inlet pipe diameter. Kurokawa's rig employs an additional blower arranged at far upstream of the divergent channel to widely change the discharge. Another method to generate a swirling flow in a conical diffuser was proposed by Kirschner et al. [7]. The swirl generator with adjustable guide vanes is installed instead of the turbine model in order to investigate different swirling flow configurations into a straight draft tube. The cone angle is 2 x 8.6°, similar with the angle of a Francis turbine draft tube cone [7].

An experimental test rig was developed to analyze the decelerated swirling flow in a conical diffuser and to evaluate the new water-injection control method [9]. The main purpose of the rig is to reproduce the hydrodynamic phenomena taking place in a conical diffuser with a decelerated swirling flow and the development of the vortex rope. The rig, developed in the Hydraulic Machinery Laboratory at Politehnica University of Timisoara is composed of the following main elements: (*i*) the main hydraulic circuit used to generate the decelerated swirling flow in the conical diffuser; (*ii*) the auxiliary hydraulic circuit needed to supply water for the jet control method. The main hydraulic circuit (showed in Figure 1 - up, with blue color) is employed to generate the main flow while the auxiliary circuit (showed in Figure 1- up with red color) help to inject water in the conical diffuser's inlet through a nozzle.

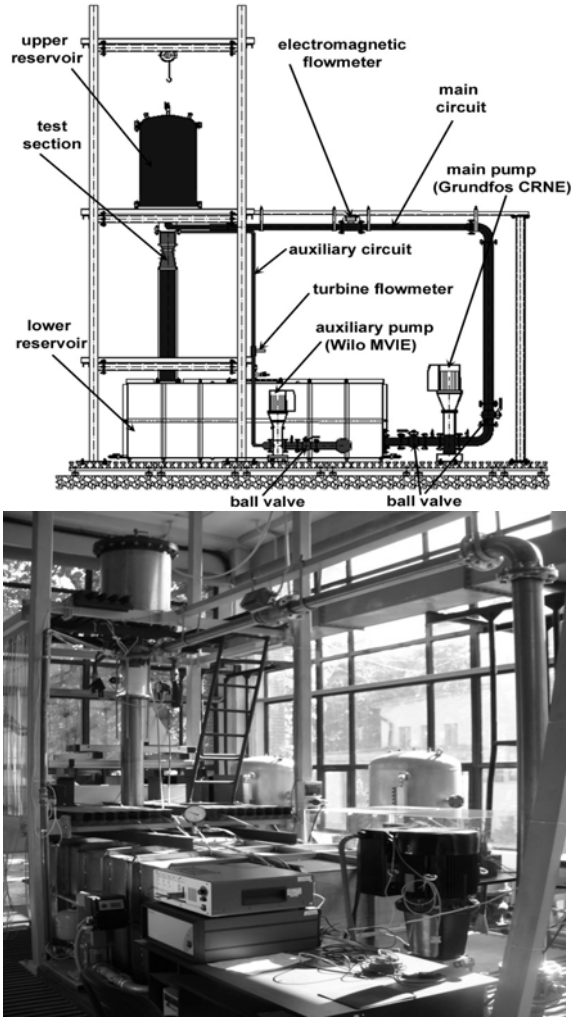

Figure 1. Experimental test rig for decelerated swirling flow, sketch (up) and picture (down).

The main part of the experimental facility is the swirl apparatus. The swirl apparatus serve to generate a swirling flow similar with the flow from a Francis turbine outlet operating at partial

discharge.

The swirl generator ends with a nozzle which allows supplying with water the jet at the inlet in the conical diffuser.

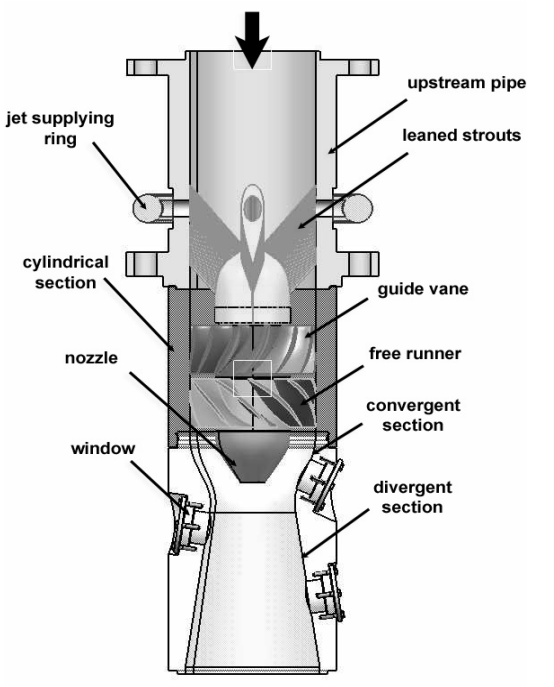

Figure 2. Sketch of the swirl apparatus with swirling flow generator and convergent-divergent test section

The test section retains only the draft tube cone from the draft tube of hydraulic turbines. Our test section was design to have a convergent part (where the flow is accelerated) and a divergent part (where the flow is decelerated) similar with the draft tube cone, having the same cone angle.

3. NUMERICAL SIMULATIONS

In order to compute the swirl apparatus we respect the following order presented in Figure 3.

Mixing interface method for coupling velocity and turbulence fields from consecutive components is used. In the mixing plane approach, each fluid zone is treated as a steady-state problem. Flow-field data from adjacent zones are passed as boundary conditions that are spatially averaged or “mixed" at the mixing plane interface. This mixing removes any unsteadiness that would arise due to circumferential variations, thus yielding a steady-state result. Despite the simplifications inherent in the mixing plane model, the resulting solution can provide reasonable approximation of the time-averaged flow field. For each domain in our computation we considered the following boundary conditionspresented in Table 1.

For numerical simulation, the ogive domain was divided into 8 symmetrical domains; being investigated only a part. By dividing the numerical domain, allows us to calculate the domain much quickly than calculation of an entire domain. The 3D numerical domain for the ogive has a structured grid with 40.000 hexahedral cells. In all investigated domains the imposed fluid is water. The guide vane has 13 fixed blades, was investigated only an interblade channel. For domain meshing was used a structured grid with 284.000 hexahedral cells.

Table 1. Boundary conditions imposed for the computational domains:

Surface	Boundary condition
inlet	Turbulence quantity and velocity components
outlet	Pressure outlet
solid	Wall
periodic	Periodicity for all qauntities

The runner has 10 blades, and for numerical simulation as in the previous case only one interblade channel is calculated. For numerical domain of the free runner we used a structured mesh with 245.000 hexahedral cells. In order to simulate the lower speeds of the runner we calculate 7 regimes.

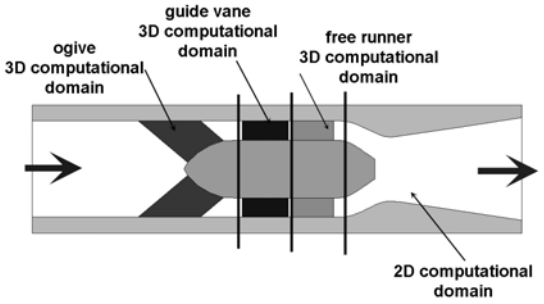

Figure 3. 3D computational domains for ogive, guide vane and free runner and 2D computational domain for the test section

First regime as shown in Table 2, is for design speed of the runner (870 rpm), and 6 regimes simulate the brake of the runner. 6 regimes were taken from 100 to 100 rpm, 300 rpm being the minimum speed which was calculated. In the below table are presented speeds of the runner which were investigated.

Table 2. Speed regimes for simulation of the runner:

No.	Speed of the runner [rpm]
1.	870 (design speed of the runner)
2.	800 (simulation at lower speeds)
3.	700 (simulation at lower speeds)
4.	600 (simulation at lower speeds)
5.	500 (simulation at lower speeds)
6.	400 (simulation at lower speeds)
7.	300 (simulation at lower speeds)

The test section domain is identical with a transversal section to the real test section from the experimental test rig. The entire domain was meshed with 30.898 hexahedral cells. Also close to the wall of the convergent divergent test section, we used a refinement of the grid. The paper will present the numerical simulation only for the swirl generator. For three-dimensional domains of the swirl generator is used Detached Eddy Simulation model (DES). From numerical simulation of the ogive, velocity profiles from the outlet of the domain were mounted as inlet conditions for the guide vane and velocity profiles from the outlet of the guide vane were mounted as inlet conditions for the runner. For the runner where imposed identical inlet conditions, and where calculated 7 regimes at different speeds as mentioned above in Table 2.

4. NUMERICAL RESULTS

From numerical simulation of the ogive, at the outlet we have the following velocity distribution.

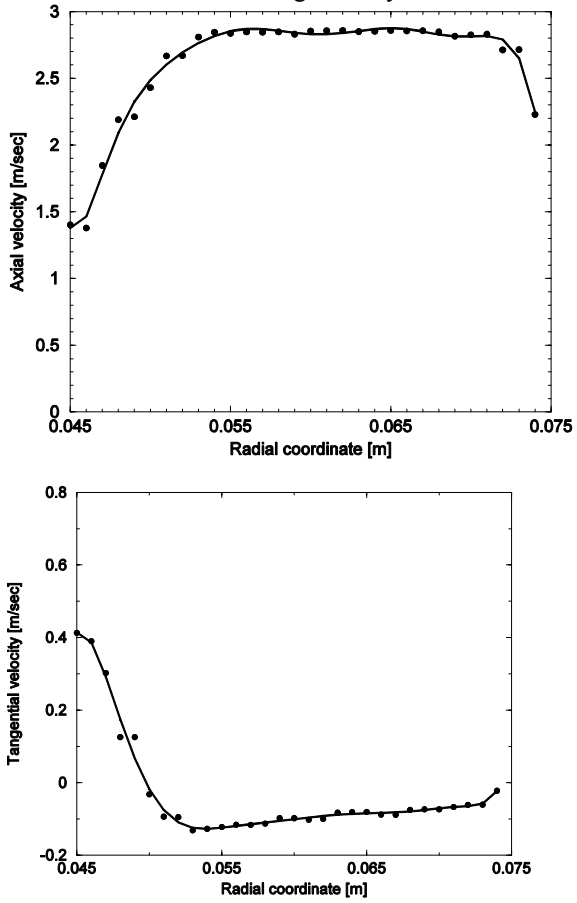

Figure 4. Axial (above) and tangential velocity component distribution at the outlet from the ogive

Knowing that the ogive has the role to sustain the swirl generator, the ogive domain will affect only the axial velocity distribution. As is observed in Figure 4, the influence of the leaned strouts, is observed close to the hub (corresponding to a radial coordinate by r=0.045 m), and close to the shroud (corresponding to a radial coordinate by r=0.075 m). A small influence of the strouts is observed in tangential velocity. This influence is observed close to the hub, at the shroud the tangential component being equal with 0.

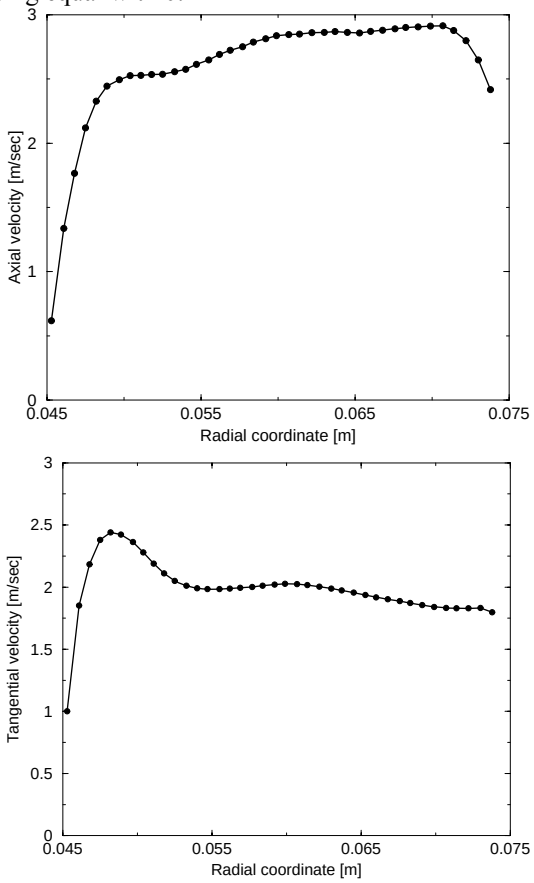

Figure 5. Velocity distribution at the outlet from the guide vane (axial and tangential velocity)

If is analysed the velocity distribution at the exit from the guide vane (Figure 5), is observed that the flow have also a tangential component. The tangential component is given deliberately in order to offer the acquired flow at the exit from swirl generator. Having calculated the velocity profiles at the outlet from the guide vane, is calculated the runner.

The runner was design that at the optimum speed (in our case 870 rpm), to operate as a Francis turbine at 70% discharge, [3],[5]. Was selected this operating point because the vortex rope developed downstream in the draft tube cone is well developed, and the pressure fluctuations generated by the vortex rope are the highest, [10].

According with Figure 6 (up) in the case of numerical simulation for the runner, the axial component at the exit from the runner has approximately a constant velocity for all 7 cases. A velocity deficit is observed close to the hub and a velocity excess is observed close to the shroud. If is analysed the tangential component at the outlet

from the runner, the velocity profiles at different lower speeds are changed dramatically. If at the optimum speed (870 rpm), we have a velocity deficit close to the hub, and a velocity excess close to the shroud with a mean velocity by 1.8 m/sec, when the speed of the runner is reduced, the mean velocity start to decrease. It reaches that at a speed of 600 rpm, the runner has the mean tangential velocity equal with 0.

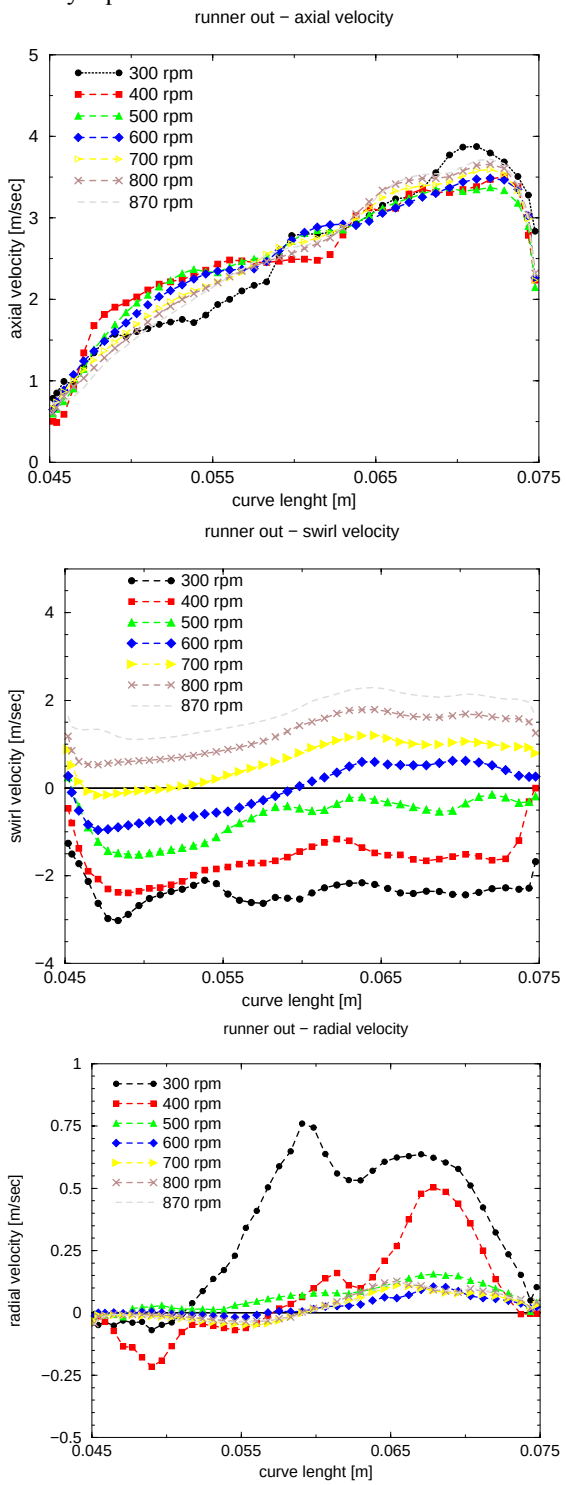

Figure 6. Axial (up), tangential (middle) and radial velocity (down) distribution at the outlet

from the runner at lower speeds

If the speed of the runner is reduced much more, the tangential component will have the mean velocity negative. More clearly if the speed of the runner is reduced we reach that a certain speed to have zero mean velocity, and if the speed of the runner is reduced much more we reach to have at the exit an opposite velocity than the case with optimum speed.

If is analysed the radial velocity component at the exit from the runner is observed that once what the speed is reduced, the velocity distribution is changed. We have this change even the radial velocity distribution at a model Francis runner is insignificant [11]. The reason for radial velocity modification in our case may be produced by the blade detaches of the runner.

Another analysis of the runner is to calculate the mechanical power generated at the shaft. The runner was design that at the optimum speed to don't produce power, but when the runner will operate at lower speeds, at the shaft is produced mechanical power. The mechanical power was calculated with formula:

$$P = M \cdot \omega [W], \ \omega = \frac{\pi \cdot n}{60} [rad / \sec] \qquad (1)$$

Where M is the torque calculated from Fluent code between the pressure side and suction side of the blade and n is the speed of the runner. The power was calculated for each investigated regime and the power of the runner depending by the speed is presented in Figure 7.

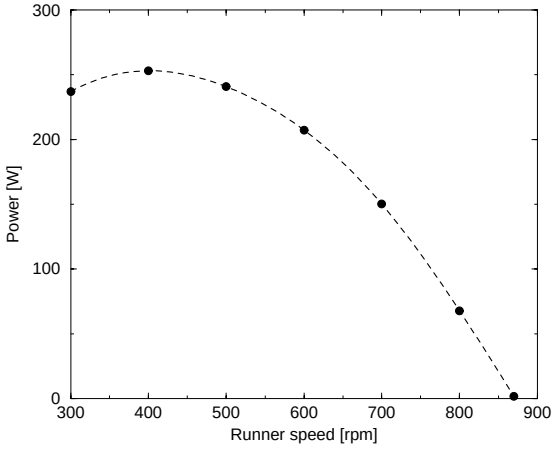

Figure 7. Power generated by the runner vs. speed

According with Figure 7, at optimum design speed, the runner does not produce power. When the speed of the runner is reduced, the power starts to increase, reaching at a maximum value by 250W at a corresponding speed by 400 rpm. If the speed of the runner is reduced over this value, the power starts to decrease. Also this decrease of the power is associated with the blade detaches.

5. DISCUSSION

In the last section, is validated a mathematical theory proposed by Resiga et al.[12]. According with this theory the so called swirl-free velocity profile at the outlet from the runner which takes into account the axial and circumferential velocity component have approximately a similar velocity profile within the full operating range. This mathematical model is suitable for early optimisation of the runner design, as it provides the swirling flow configuration at runner outlet without actually computing the runner. By optimising the parameterized swirl-free velocity profile one can achieve through the inverse design approaches the most suitable runner blades configuration at the trailing edge.

The main hypothesis concerning the swirl-free velocity profile introduced above as an alternative to the relative flow angle at runner outlet is that $v_{sf}(r)$ is practically unchanged as the operating regime spans the whole operating range of the turbine.

Having the computed velocity profiles at the outlet of our free runner, we will calculate this parameter in order to determine if this theory is validated on our swirl generator.

The analysis of our swirl generator starts with the fundamental equation of turbomachines, written for a hydraulic turbine as.

$$\eta(\rho Q)(gH) = \\ = \int_{S_1} \overbrace{(\omega R V_\theta)\rho V_r dS_1}^{M_1} - \int_{S_2} \overbrace{(\omega R V_\theta)\rho V_z dS_2}^{M_2} \qquad (2)$$

In the left-hand side we have the hydraulic power written as the product of the mass flow rate ρQ and specific energy gH, multiplied by the hydraulic efficiency η. In the right hand side we have the rate at which the fluid does work on the runner, which by Newton's second law applied to the moment of forces is equal to the difference in the flux of moment of momentum between cross-sections upstream the free runner S_1, and downstream the runner S_2, respectively. Obviously, when computing the flux of moment of momentum upstream and downstream the runner respectively, M_1 and M_2, we use the axial velocity V_{1r} and V_{2z} respectively. The circumferential velocity upstream the runner is $V_{1\theta}$, while downstream the runner we have $V_{2\theta}$.

The above equation can be written in dimensionless form by introducing the following coefficients.

$$\phi = \frac{\rho Q}{\rho\left(\omega R_{ref}\right)\pi R_{ref}^2} \qquad (3)$$

Where ϕ is defined as discharge coefficient, having R_{ref} shroud radius from the swirl generator.

$$m_2 = \frac{M}{\rho\left(\omega R_{ref}\right)^3 \pi R_{ref}^2} \qquad (4)$$

where, m_2 is defined as the flux of moment of momentum coefficient at the outlet from the runner. From numerical simulation of the runner from the swirl apparatus at lower speeds we have the variation of flux of moment of momentum coefficient presented in Figure 8.

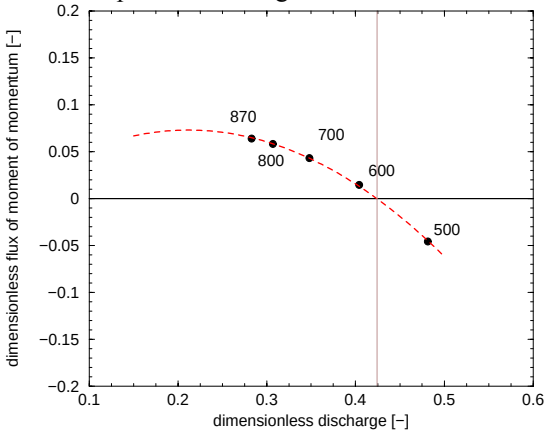

Figure 8. Dimensionless flux of moment of momentum downstream the runner depending by the discharge coefficient

This coefficient is directly related to discharge and circumferential velocity downstream the runner. We observe that at the optimum design speed, 800, 700 and 600 rpm, the circumferential velocity at the exit of the runner has a positive value and if we continue to reduce the speed of the runner, the circumferential velocity will have a negative value and the swirl counter-rotates with respect to the runner. Also from this graph is possible to notice the speed of the runner were the flux of moment of momentum coefficient vanishes. At this operating point the circumferential velocity profile will have the mean value equal with zero, at the outlet of the runner being only the axial component.

For turbine runners with fixed pitch blades, the swirling flow at the runner outlet must satisfy the kinematic constraints given by the runner blades geometry. Accordingly with Figure 9, the velocity triangle provides the kinematic constraint corresponding to the relative flow angle β_2. This angle is changing along the radius, corresponding to the blade geometry from hub to shroud. Figure 9 shows three particular configurations of the velocity triangle, with the relative velocity kept on the same direction given by β_2. Also the transport velocity ωR remains the same for all three cases. The absolute circumferential velocity $V_{2\theta}$ has the same direction as the transport velocity at low discharge and is in opposite direction with the transport velocity, and the swirl counter rotates with respect to the runner at large discharge case. In-between we can always identify a regime where the absolute circumferential velocity vanishes, $V_{2\theta}$ =0.

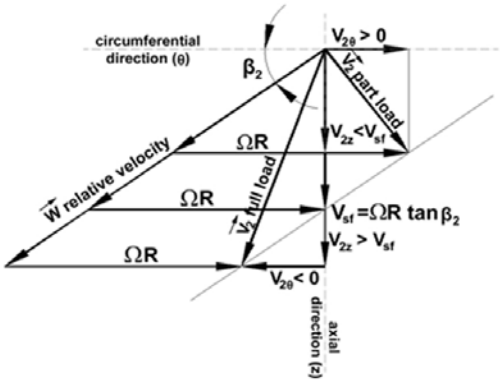

Figure 9. Velocity triangle downstream the runner, for variable operating regimes.

The swirl-free velocity component is directly related to the relative flow angle, $V_{sf} = \omega R tan\beta_2 \Rightarrow tan\beta_2 = V_{sf} / \omega R$. And for an arbitrary operating regime we have.

$$\frac{V_{2z}}{\omega R - V_{2\theta}} = \tan\beta_2 = \frac{V_{sf}}{\omega R} \quad (5)$$

Thus the swirl-free velocity can be written as.

$$V_{sf} = \frac{\omega R V_{2z}}{\omega R - V_{2\theta}} \quad (6)$$

Eq. 6, written in dimensionless form:

$$v_{sf} = \frac{r v_{2z}}{r - v_{2\theta}} \quad (7)$$

Figure 10 shows the variation of swirl-free velocity component for all investigated regimes of the runner from our swirl apparatus. It can be seen that the swirl-free velocity is reasonably similar for all regimes. The exception is for speeds of the runner by 300 and 400 rpm where the velocity is not identical. For these regimes we have detaches of the flow from the blade, and also this is reflected in swirl-free velocity.

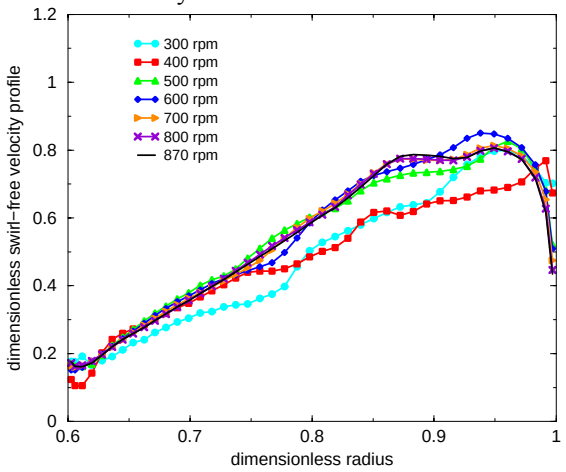

Figure 10. The swirl-free velocity profile at the runner outlet at lower speeds

From Figure 10 is concluded that the theory proposed by Resiga et al. [12], for the computation of the swirling flow at the Francis runner outlet with swirl-free velocity is correct, the velocity v_{sf} remaining constant at any operating regime.

6. CONCLUSIONS

The paper presented a numerical analysis of a swirling flow generator at lower speeds. The main goal was to analyse the velocity profiles at the outlet. The swirl generator contains a free runner and was numerically investigated at the design speed and at 6 lower speeds. From the velocity profiles is observed that the axial component of the velocity at the exit from the runner remain constant. The major modification when the runner works at lower speeds is observed in tangential velocity component. Once the runner speed decrease, the tangential velocity also decrease. So the runner reach that a lower speed to have at the outlet only the axial component, the circumferential velocity vanishing. At the end of the paper, is validated a mathematical theory proposed by Resiga et al.[12]. According with this theory the so called swirl-free velocity profile at the outlet from the runner which takes into account the axial and circumferential velocity component have approximately a similar profile for all operating regimes. The theory was validated also on our swirl generator, the swirl-free velocity having a similar profile for all investigated regimes. Knowing the axial and circumferential velocity profile from the outlet of the runner (therefore the swirl-free velocity), the proposed theory will help at the optimisation of swirling flow ingested by the turbine's draft tube before designing the runner. The theory connects the swirl from the inlet in the draft tube cone with the swirl from the hydraulic turbine, knowing that the efficiency hill-chart is actually driven by the hydraulic losses in the draft tube.

ACKNOWLEDGEMENTS

This work was supported by a grant of the Romanian National Authority For Scientific Research, CNCS – UEFISCDI, project number PN-II-RU-PD-2011-3-0165.

REFERENCES

[1] Vu, T.C. and Retieb, S., 2002, "Accuracy assessment of current CFD tools to predict hydraulic turbine efficiency hill chart", *Proceedings of the XXIst IAHR Symposium on Hydraulic Machinery and Systems,* Laussane, Switzerland, pp. 1-6.

[2] Susan-Resiga, R., Muntean, S., Bosioc, A., Stuparu, A., Milos, T., Baya, A., Bernad, S., Anton L.E., 2007, "Swirling flow apparatus and test rig for flow control in hydraulic turbines discharge cone", *Proceedings of 2nd IAHR International Meeting of the Workgroup on*

Cavitation and Dynamic Problems in Hydraulic Machinery and Systems, Tom 52(66), Fascicola 6, pp. 203-207. Scientific Bulletin of the Politehnica University of Timisoara, Transactions on Mechanics.

[3] Susan-Resiga, R., Muntean, S., Tanasa, C., Bosioc, A.I., 2008, "Hydrodynamic design and analysis of a swirling flow generator", *4th German-Romanian Workshop of Vortex Dynamics in Hydraulic Machinery*, Stuttgart, Germany, pp. 1-16.

[4] Susan-Resiga, R., Vu, T., Muntean, S., Ciocan, G., and Nennemann, B., 2006, Jet control of the draft tube vortex rope in Francis turbines at partial discharge. *Proceedings of the 23rd IAHR Symposium on Hydraulic Machinery and Systems*, Yokohama, Japan, (p. 192).

[5] Susan-Resiga, R., Muntean, S., 2008, "Decelerated Swirling Flow Control in the Discharge Cone of Francis Turbines" *Proceedings of the Fourth Symposium on Fluid Machinery and Fluid Engineering*, Beijing, China, Springer, pp. 89-96.

[6] Kurokawa, J., Kajigaya, A., Matusi, J., and Imamura, H., 2000, "Suppression of Swirl in a Conical Diffuser by Use of J-Groove," *Proceedings of the 20th IAHR Symposium on Hydraulic Machinery and Systems*, Charlotte, North Carolina, Paper DY-01.

[7] Kirschner, O., Schmidt, H., Ruprecht, A., Mader, R., and Meusburger, P., 2010, "Experimental investigation of vortex control with an axial jet in the draft tube of a model pump-turbine", *Proceedings of the 25th IAHR Symposium on Hydraulic Machinery and Systems in IOP Conf. Series: Earth and Environmental Science*, Timisoara, Romania, Vol. 12, p. 012092.

[8] Avellan, F., 2000, "Flow investigation in a Francis draft tube: the FLINDT project", *Proceedings of the 20th IAHR Symposium on Hydraulic Machinery and Systems*, Charlote, USA, pp. DES-11.

[9] Bosioc, A.I., Tanasa, C., Muntean, S., Susan-Resiga, R., 2010, "Pressure recovery improvement in a conical diffuser with swirling flow using water jet injection", *Publishing House of the Romanian Academy, Proceedings of the Romanian Academy, Series A: Mathematics, Physics, Technical Sciences, Informational Science*, Vol. 11, Number 3, pp. 245-252.

[10] Jacob, T., 1993, "Evaluation sur modele reduit et prediction de la stabilite de fonctionnement des turbines Francis", *Phd thesis*, Ecole Politehnique de Lausanne, Switzerland.

[11] Tridon, S., Barre, S., Ciocan, G.D., Tomas, L., 2010, "Experimental analysis of the swirling flow in a Francis turbine draft tube: Focus on radial velocity component determination", *European Journal of Mechanics B/Fluids*, Vol. 29, pp. 321-335.

[12] Susan-Resiga, R., Muntean, S., Avellan, F., Anton, I., 2011, "Mathematical modelling of swirling flow in hydraulic turbines for the full operating regime", *Applied Mathematical Modelling*, Vol. 35, pp. 4759-4773.